# CBIR Efficiency Enhancement using Local Features Algorithm with Hausdorff Distance

STELLA VETOVA, IVO DRAGANOV
Radiocommunications and Videotechnologies Dept.
Technical University of Sofia
Sofia
BULGARIA
vetova.bas@gmail.com, idraganov@tu-sofia.bg

IVAN IVANOV
Telecommunication Technologies Dept.
Higher School "College of Telecommunications and Post"
Sofia
BULGARIA
ivanivanov@hctp.acad.bg

VALERI MLADENOV
Theoretical Electrical Engineering Dept.
Technical University of Sofia
Sofia
BULGARIA
valerim@tu-sofia.bg

*Abstract:* - The paper below discusses the pros and cons of the local and global features in CBIR. To this end, four CBIR algorithms are designed and studied in terms of effectiveness. Two of them are based on local features extraction and the similarity is computed through Hausdorff distance or Euclidean distance respectively. The rest of the algorithms use global features extraction and the same two similarity distance metrics. For the feature extraction the Dual-Tree Complex Wavelet transform (DT CWT) is applied. The conducted experiments show that the local Features Algorithm with Hausdorff distance (LFAH) which was recently proposed in our previous study demonstrates better results in terms of effectiveness.

*Key-Words:* - CBIR; DT CWT; image decomposition; global and local features; Hausdorff distance

## 1 Introduction

The modern world of high technologies leads to large-scale information. Its storing and processing need more and more computational memory, storage space, graphical resources, and so on. More than twenty years the world research society has been focused on the problem of CBIR algorithms efficiency and effectiveness. The area of Content-Based Image Retrieval is widely applicable in the fields of education, medicine, culture, heritage, GIS, satellite images, architecture, criminology, and others [1].

There are a good many methods designed for the purposes of Content-Based Image Retrieval. One of the most popular and recently used technique is the wavelet transform [2]. It is remarkable for its property to produce spatial and frequency image description. The obtained feature vectors raise both the precision of the retrieved result as well as the CBIR algorithm execution speed. Besides, the modern wavelet transform concerns directivity [3], which makes it more attractive in practical aspect. Thus, the wavelet technology turns out to be effective and approprate for a wide scope of social life activities. Regardless of the numerous designed techniques developed throughout the years worldwide, there is still no final solution found regarding the CBIR effectiveness and efficiency problem.

There are two CBIR effectiveness evaluation approaches: the non-rank evaluation approach and the rank evaluation one. In the first case, the CBIR system effectiveness is evaluated based on the relevant retrieved images and the number of all relevant images found in the test image database (IDB). The classical measures applied in the non-

rank evaluation are precision and recall according to formulae (1) and (2):

$$Precision = \frac{\left|relevant \bigcap retrieved\right|}{\left|retrieved\right|}, \quad (1)$$

$$Recall = \frac{\left|relevant \bigcap retrieved\right|}{\left|relevant\right|}. \quad (2)$$

The rank evaluation approach uses a technique to estimate rank positions where relevant images are retrieved. The measures used most often are average precision and average recall based on the precision and recall values of all queries results. Usually, the rank evaluation approach uses a pattern of 5, 10, 20 or 50 rank positions *(k)* [4].

Rank *(k)* index presents the rank position of the retrieved image and is defined as follows [5]:

$$Rank\,(k) = \begin{cases} R(k) & if R(k) \le K(q) \\ (K+1) & if R(k) > K(q) \end{cases}. \quad (3)$$

Berman and Shapiro [6] use the rank of the best match where they estimate the relevance of the retrieved images in the first 50 images on the screen or in the first 500 which is the maximum images during browsing.

Gargi and Kasturi [7] use the average rank of relevant images. However, this measure depends on the test IDB size and the number of the retrieved relevant images for a query which causes difficulty in its interpretation. To overcome this drawback, Muller et al. [4] propose a normalized average rank $\tilde{Rank}$ (4):

$$\tilde{Rank} = \frac{1}{NN_R}\left(\sum_{i=1}^{N_R} R_i - \frac{N_R(N_R-1)}{2}\right) \quad (4)$$

where $R_i$ is the rank at which the i[th] relevant image is retrieved.

The $\tilde{Rank}$ varies in the scope of [0,1]. The effectiveness is the highest when $\tilde{Rank}$ reaches the value 0. Quite the opposite, when it gets closer to the value 1, the effectiveness gets worse.

This paper presents a comparative analysis of the effectiveness between four CBIR algorithms based on local and global features extracted through DT CWT. It is structured as follows. Section II discusses in short the Dual-Tree Complex Wavelet Transform as a filter bank (FB) structure, running process and applications. Section III is divided into three subsections. The first one introduces CBIR effectiveness evaluation rank measures. The second one describes four algorithms for Content–Based Image Retrieval using the Dual-Tree Complex Wavelet Transform. The third one depicts the accomplished test experiments and the experimental results. Section IV presents the final conclusion followed by the description of four algorithms proposed by our team using DT CWT.

## 2 The Dual-Tree Complex Wavelet Transform

The Dual-Tree Complex Wavelet Transform (DT CWT) is designed in 1998 by Nick Kingsbury. Its construction uses one binary wavelet tree for the real part and another one for the imaginary part of the Complex Transform, both consisting of highpass and lowpass filters. The Discrete Wavelet Transform is performed on each of the trees. Thus, DT CWT produces an analytic signal with the following properties: smooth non-oscillating magnitude; nearly shift-invariant magnitude; significantly reduced aliasing effect; directional wavelets in higher dimensions.

DT CWT is a biorthogonal transform, which uses linear-phase filters, satisfying the Perfect Reconstruction (PR) condition [8] and which produces approximately analytic signal:

$$\Psi(t) := \Psi_R(t) + j\Psi_J(t) \quad (5)$$

where $\Psi_R(t)$ and $\Psi_J(t)$ are the wavelets generated by the two Discrete Wavelet Transforms (DWTs).

To reach a nearly shift-invariant wavelet transform, one of the two lowpass filters has to be nearly half-sample shift to the other:

$$J_0(k) \approx R_0(k-0.5) \Rightarrow \Psi_J(t) \approx H\{\Psi_R(t)\}. \quad (6)$$

In its practical application DT CWT is used in two-dimensional space for image processing. It is suitable for edge and surface detection. 2D DT CWT has application in image segmentation [9], motion estimation [10], texture analysis and synthesis [11], feature extraction [12], [13].

# 3 CBIR Algorithms Effectivenes Evaluation and Experimental Results

## 3.1 CBIR effectiveness evaluation

Content-Based Image Retrieval is a technology for digital image classification by visual content. The CBIR system evaluation is based on the usage of test image databases such as Wang database [14], [15], [16], [17], the COREL database [18], [19], Brodatz texture database [20], Photometric Texture database [21], etc. Each of the test databases is defined as a set of *I* images and *q* queries. A query is a submitted image from the set (to the system). After the query processing, the system retrieves images from the database with similar visual content by rank. The item-ranking approach is applied for the CBIR effectiveness evaluation. One of the most often used measures for this are the Mean Average Precision *(MAP)* (8) and the Averaged Normalized Modified Retrieval Rank *(ANMRR)* (12) which are considered to be the most suitable for CBIR systems [22]. *MAP* computes on the base of the Average Precision *(AP)* in the following order:

$$AP(q) = \frac{1}{NG(q)} \sum_{k=1}^{NG(q)} P_q(R_k) \qquad (7)$$

where q is the query; *NG(q)*–a set of retrieved images for *q*;

$R_k$ – Recall in *k*-th relevant retrieved image.

Hence:

$$MAP = \frac{1}{Q} \sum_{q \in Q} AP(q) \qquad (8)$$

where Q is a set of *q* queries.

*MAP* varies in the range of [0,1]. The closer it approaches the value 1, the greater number of relevant images the evaluated CBIR system retrieves, and vice versa.

In contrast, covering the range of [0,1], the more the *ANMRR* values come closer to 1, the greater number of irrelevant images are retrieved by the CBIR system. *ANMRR* computes, using the following formulae order:

$$AVR(q) = \sum_{k=1}^{NG(q)} Rank(k) \Big/ NG(q) \qquad (9)$$

where *Rank (k)* is the rank of the first $\kappa$ relevant images, retrieved by the query; *NG (q)* – number of the retrieved relevant images for the query *q*;

$$MRR(q) = AVR(q) - 0.5 \times [1 + NG(q)], \qquad (10)$$

$$NMRR(q) = \frac{MRR(q)}{1.25 \times K - 0.5 \times [1 + NG(q)]}, \qquad (11)$$

$$ANMRR = \frac{1}{Q} \sum_{q=1}^{Q} NMRR(q) \qquad (12)$$

An advantage of both metrics (*MAP* and *ANMRR*) is the combination of the correlated precision and recall metrics. On the other hand, they do not take into account the size of the test image database which may lead to incorrect system effectiveness evaluation and the system behavior would be impossible to be predicted.

The classical item-ranking approach for CBIR effectiveness evaluation includes the precision-recall curves $P_k$ vs $R_k$. Each of the points is computed on a recall cut-off value. The precision-recall curve describes the behavior of the CBIR system above a preliminarily chosen rank threshold. Precision and Recall measures are computed according to formulae (13) and (14):

$$Precision_{AVR} = \frac{1}{Q} \sum_{i=1}^{Q} Precision_i, \qquad (13)$$

$$Recall_{AVR} = \frac{1}{Q} \sum_{i=1}^{Q} Recall_i \qquad (14)$$

where *i* is the treated image.

There are two types of tasks, which CBIR systems may implement. The first one is the precision-oriented task and the second one – the recall-oriented [22]. The precision-oriented task concerns the cases when the system achieves higher relevance precision in the first *K* ranks on analogy of the Web space. On the other hand, the recall-oriented task requires the retrieval of all relevant images from the test database. This scenario is applicable in the area of medicine.

To compare the effectiveness of different CBIR systems where the database and scope are constant parameters, it is recommended to use single value effectiveness measures such as *AP* and *Accuracy*:

$$Accuracy = \frac{(Precision + Recall)}{2} \qquad (15)$$

Furthermore, to evaluate the effectiveness of a CBIR system it is necessary to compute the average retrieval speed ($t_{AVR\ Im\ Ext}$) and the average number of the retrieved images ($I_{AVR\ RTR}$) as follows:

$$t_{AVR\,\mathrm{Im}\,Ext} = {}^{1}\!/_{Q} \sum_{i=1}^{Q} t_{\mathrm{Im}\,Ext_i}\ ,\mathrm{sec} \qquad (16)$$

where: $Q$ – a set of queries $q$;

i – treated image.

$$I_{AVR\,RTR} = {}^{1}\!/_{Q} \sum_{i=1}^{Q} I_{RTR_i}\ . \qquad (17)$$

### 3.2 Local and global features extraction

Fig. 1 presents a CBIR system architecture realized in this research. It consists of an offline subsystem and an online subsystem. The first one deals with the generation of the test images feature vectors DB and the latter with the generation of the query image feature vector. Both subsystems implement five common processes such as: Image reading from the test DB; Image scaling; Image conversion from RGB into greyscale space; Image division into 8x8 blocks and DT CWT feature extraction.

First, each image is read as a matrix *A[i,j]* with rows *i* and columns *j* which locate the position of the pixels. Then, each image is scaled into 256 x 256 pixels, applying bicubic interpolation through formula (18) as follows:

$$u(s) = \begin{cases} (a+2)|s|^3 - (a+3)|s|^2 + 1 & 0 < |s| < 1 \\ a|s|^3 - 5a|s|^2 + 8a|s| - 4a & 1 < |s| < 2 \\ 0 & 2 < |s| \end{cases} \qquad (18)$$

where $a$=-0.5.

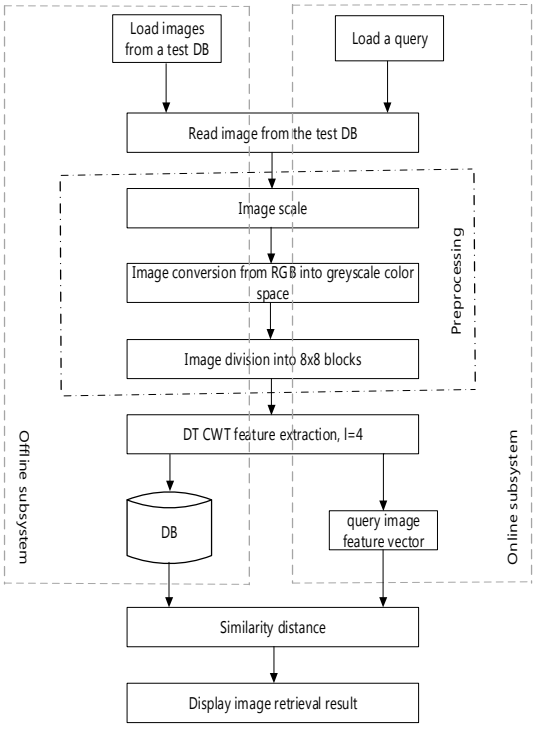


Fig. 1. CBIR system architecture

On the third stage, images are converted from RGB into greyscale color space through a weighted sum ( $C$ ) according to (19):

$$C[i,j] = 0.2989[i,j]R + 0.5870[i,j]G + 0.1140[i,j]B \qquad (19)$$

Fourth, each image matrix *C[i,j]* (where i=j=256) is divided into 64 square matrices $C_n^{'}[i,j]$ (where $n = 1 \div 64$) each 32 x 32 pixels in size. Each submatrix presents a separate subimage.

Finally, on each subimage $C_n^{'}$ DT CWT at the fourth transform level (*l=4*) is applied. As a result, there are 16 wavelet coefficients: 8 detail coefficients and 8 approximate coefficients.

Thus, the extracted feature vectors of the first images are stored in a database designed in advance. To display similar images a similarity distance between the feature vectors from the DB and the submitted query image feature vector is implemented.

The paper includes a comparative analysis of effectiveness of four different algorithms. The first two of them, the **L**ocal **F**eatures **A**lgorithm with **H**ausdorff distance (LFAH) which was developed in our prior work [24] and the **L**ocal **F**eatures

**A**lgorithm with **E**uclidean distance (LFAE) are based on the local feature extraction, using image division process described in short above. The applied similarity distance is Hausdorff distance and Euclidean distance respectively.

The second two of the algorithms, Global **F**eatures **A**lgorithm with **H**ausdorff distance (GFAH) and the **G**lobal **F**eatures **A**lgorithm with **E**uclidean distance (GFAE) use global feature extraction with Hausdorff distance or Euclidean distance. These algorithms run according to Fig. 1, excluding the process of image division. Thus, DT CWT runs on the entire test images, extracting the feature vector.

### 3.3 Experimental results

To the end of the discussed algorithms, Wang image test database, containing 1000 RGB images was used. The database is organized in 10 semantically different groups, each of 100 images as follows: nature, architecture, vehicles, dinosaurs, elephants, flowers, horses, food, Africa and social life. The images differ in size of *256x384px* and *384x256px* in JPEG format.

The four algorithms are tested using the software for mathematical and engineering computation Matlab R 2008b on a personal computer with the following configuration: Intel (R) Core (TM) 2 Duo 2,40 GHz, 32-bit Operating System.

For the purpose of the implemented experiments is the effectiveness evaluation of the four algorithms and a comparative analysis between them in terms of local and global features. The experiments are based on a pattern of the first ten retrieved images after the submission of the query *q*. For the successful experiment implementation there must be at least two semantically relevant images in the pattern. Based on the latter, the measures *Precision* (13) and *Recall* (14) are computed as well as the rank and the image relevance are defined. Such an experiment is implemented for five queries *q* for each of the ten test image categories. Using the entire set of *Precision* and *Recall* results, 11-point interpolation is computed. It depicts the algorithm effectiveness through a *Precision x Recall* curve.

Fig.2 illustrates the LFAH and LFAE effectiveness. It reveals that the first one demonstrates higher effectiveness compared to the second in the area between *Recall=0* and *Recall<0.3* as well as in the areas located between *Recall>0.3* and *Recall=1*. In *Recall= 0.3* both algorithms have equal value for *Precision* criteria. For the rest of the areas LFAH reaches higher values for *Precision* and has a higher capability to retrieve relevant images in the positions with higher rank than the second one. For the values *Recall>0.3* the differences between the two algorithms gradually rise. The greatest difference is in the area between *Recall=0.5* and *Recall=0.9*.

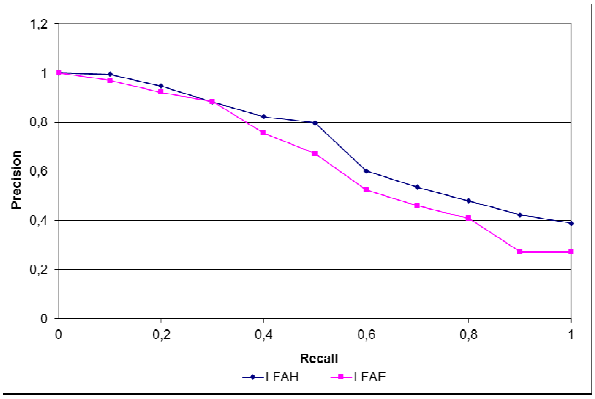


Fig. 2. Precision x Recall curve for LFAH and LFAE

Fig. 3 represents *Precision x Recall* curves for GFAH and GFAE. They show that GFAE is remarkable for higher effectiveness retrieving only relevant images in positions with the highest rank. On the contrary, GFAH retrieves considerable number of irrelevant images for these rank positions. The alteration of the two curves is similar as the maximum difference is in *Recall=0.5*. From both algorithms GFAH retrieves more irrelevant images than GFAE.

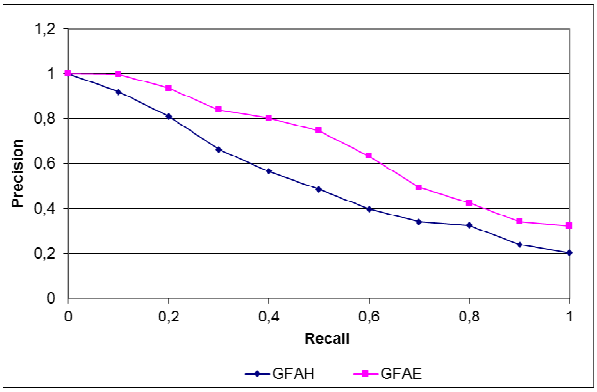


Fig. 3. Precision x Recall curve for GFAH and GFAE

On the base of the implemented analysis of Fig. 2 and Fig. 3 we conclude that LFAH and GFAE are the algorithms with higher effectiveness. The

comparison between them gives the opportunity to make an assessment. Their effectiveness is presented graphically on Fig. 4 through *Precision x Recall* curve. It shows that both algorithms have close effectiveness with minimal advantage for LFAH. The only area where GFAE is slightly better is *Recall=0.6*. This allows us to conclude that comparing the four presented algorithms based on *Precision* criteria, LFAH demonstrates the highest effectiveness.

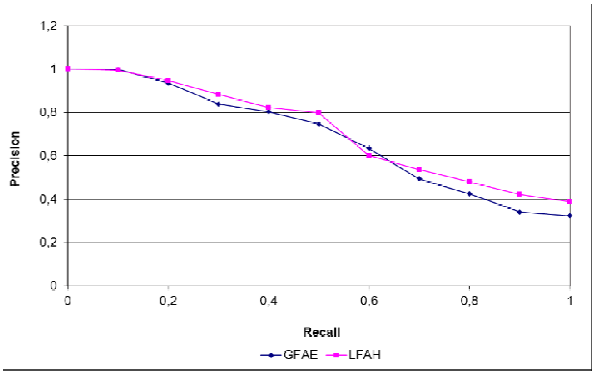


Fig. 4. Precision x Recall curve for GFAE and LFAH

To compute *Recall* we use the ratio of the number of the retrieved relevant images to all the images, belonging to the query-image category. Thus, we also estimate the semantics of the generated result.

Apart from the *Precision x Recall* curve, a comparative analysis and effectiveness evaluation of the four algorithms is carried out based on the average values of: $t_{ImExt}$, $I_{AVR\ RTR}$, $Precision_{AVR}$, $Recall_{AVR}$, *ANMRR, Accuracy* and *MAP* tabulated in Table 1.

TABLE I. AVERAGE VALUES FOR $T_{IMEXT}$, $I_{AVR\ RTR}$, PRECISION $_{AVR}$, $RECALL_{AVR}$, ANMRR, ACCURACY AND MAP

| Ctiterion | LFAH | LFAE | GFAH | GFAE |
|---|---|---|---|---|
| **Retrieval time (s)** | 0,47 | 0,42 | 0,57 | 0,34 |
| **Number of retrieved images** | 22,24/ 1000 | 21,06/ 1000 | 29,14/ 1000 | 17,36/ 1000 |
| **Precision** | 56,26% | 55,35% | 47,92% | 53,27% |
| **Recall** | 11,08% | 10,76% | 12% | 9,68% |
| **ANMRR** | 0,210 | 0,231 | 0.249 | 0,207 |
| **Accuracy** | 33,67% | 33,06% | 29,96% | 31,47% |
| **MAP** | 82,60% | 81,28% | 78,16% | 80,86% |

The GFAE has the highest values for $t_{ImExt.}$ This is due to the technological simplicity of the algorithm and the plain mathematical formula of the Euclidean distance. In comparison, the distance computation, using Hausdorff distance requires a longer time period.

$I_{AVR\ RTR}$ criterion is calculated according to the total number retrieved images. The result shows that GFAH demonstrates the highest percent retrieved images at the expense of *Precision*. This fact is caused by the GFAH ability to retrieve a considerable number of irrelevant images which decreases the precision of the final result.

On the contrary, GFAE has the lowest percent of retrieved images. Analyzing its *Precision* values, it is clearly seen that it has the ability to retrieve a greater number of relevant images and a smaller number of irrelevant images. LFAH demonstrates similar behavior. Its average values indicate that the algorithm retrieves a greater number of relevant images than the irrelevant ones.

For the criterion Accuracy, LFAH has the highest value. This result is based on the higher *Precision* value than the Recall one. LFAE has close values for *Accuracy* but the *Precision* value is lower than the LFAH one.

The GFAE algorithm has the best ANMRR values followed by the LFAH. The obtained results prove the ability of LFAE and GFAH to retrieve irrelevant images in high rank positions.

As for *MAP* measure, LFAH is notable for the highest values and GFAH for the lowest ones.

Table 2 and 3 present the average *Precision* and *Recall* for four compared CBIR methods as follows: Local Histogram Method, Mean Segment Method, Variance Segment Method, LFAH [23]. Fig. 5 depicts the retrieved results for precision and recall for all image collection groups.

A summarized estimation on the comparison data shows that the proposed LFAH demonstrates best recognition results for a given query for image categories “social life”, “architecture”, “dinosaurs”,

"elephants", "flowers", "horses", "nature", and "food".

Compared to the Local Histogram Method and the Variance Segment Method, the Mean Segment Method retrieves best results for the image groups: "social life", "busses", "dinosaurs", "elephants", "roses", and "horses". The Local Histogram Method demonstrates best Precision results for the four presented methods in the category "Africa". For "Nature" the Variance Segment Method generates the most relevant images.

According to *Precision* measure, LFAH retrieves most relevant images when they have homogeneous background. This property makes it most appropriate to be embedded in CBIR systems for recognition of the described type of images. Furthermore, the retrieved results for collection image groups "nature", "architecture", "food", and "dinosaurs" prove the LFAH ability to detect by texture. Similarly, the results for "flowers", "elephants", and "horses" indicate the ability to detect by shape.

The obtained Precision and Recall results show that LFAH is appropriate for CBIR systems with precision-oriented task.

TABLE II. AVERAGE PRECISION AND RECALL FOR LOCAL HISTOGRAM METHOD AND MEAN SEGMENT METHOD

| | **Local Histogram Method** | | **Mean Segment Method** | |
|---|---|---|---|---|
| **Measure** | **Precision %** | **Recall %** | **Precision %** | **Recall %** |
| **Average** | 25.46 | 5.1 | 33.385 | 6.677 |

TABLE III. AVERAGE PRECISION AND RECALL FOR VARIANCE SEGMENT METHOD AND LFAH

| | **Variance Segment Method** | | **LFAH** | |
|---|---|---|---|---|
| **Measure** | **Precision %** | **Recall %** | **Precision %** | **Recall %** |
| **Average** | 36.11 | 6.212 | 56.49 | 5.7 |

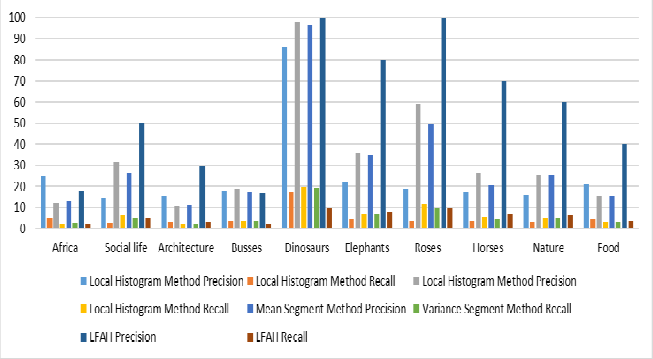


Fig. 5. Precision and Recall ratio by image categories for the compared methods

## 4 Conclusion

The implemented experiments highlight LFAH and GFAE algorithms being the most efficient from the tested ones using local and global features groups. It is concluded that LFAH requires a longer time period for image retrieval than GFAE. The reasons are founded on the executed opperations on image division, features extraction from the subimages and Hausdorff distance computation which needs a greater number of operations than Euclidean distance. The obtained average values as well as the analyzed *Precision x Recall* curve show that LFAH demonstrates best ability for relevant image retrieval in the highest rank positions. Besides, according to a comparative analysis of four CBIR methods such as Local Histogram Method, Mean Segment Method, Variance Segment Method and the proposed LFAH, the last one generates most precise results.

*References:*

[1] S. Banuchitra, Dr. K. Kungumaraj, "A Comprehensive Survey of Content Based Image Retrieval Technique," *International Journal Of Engineering And Computer Science*, vol. 5, issues 8, 2016, pp. 17577-17584.

[2] V. Noutson, D. Argialas, P. Michalis, "Edge detection of manmade objects using wavelets in high resolution satellite images," *ASPRS Annual Conference*, 2007.

[3] G. Strang, T. Nguyen, *Wavelets and Filter Banks*, Wellesley-Cambridge Tress, 1998.

[4] H. Muller, W. Muller, D. Squire, S. Maillet, and T. Pun, "Performance Evaluation in Comtent-Based Image Retrieval: Overview and Proposals," *Pattern recognition Letters*, vol. 22, issue 5, 2001, pp. 593-601.

[5] G. Park, Y. Baek, H. Lee, "A Ranking Algorithm Using Dynamic Clustering for Content-Based Image Retrieval," *International Conference on Image and Video Retrieval*, 2002, pp. 328-337.

[6] A. Berman, L. and Shappiro, "Efficient content-based retrieval: Experimental results," *CBA*, 1999, pp. 55-61.

[7] U. Gargi, and R. Kasturi, "Image database querying using a multi-scale localized color representation," *CBA*, 1999, pp. 28-32.

[8] I. Selesnick, R. Baraniuk, and N. Kingsbury, "The dual-tree complex wavelet transform", *IEEE Signal Processing Magazine*, November, 2005, pp. 123-151.

[9] C. W. Shaffrey, N. G. Kingsbury, and I. H. Jermyn, "Unsupervised image segmentation via Markov trees and complex wavelets", *In Proceedings of IEEE International Conference on Image Processing*, 2002, pp. 801-804.

[10] J. Magarey, and N. Kingsbury, "Motion estimation using a complex-valued wavelet transform", *IEEE Trans. on Signal Processing, special issue on wavelets and filter banks*, vol. 46, No 4, April 1998, pp 1069-84.

[11] P. R. Hill, D. R. Bull, and C. N. Canagarajah, "Rotationally invariant texture features using the dual-tree complex wavelet transform", *in Proceedings of IEEE International Conference on Image Processing,* 2002, pp. 901-904.

[12] B. Liao, and F. Peng, "Rotation-invariant texture features extraction using dual-tree complex wavelet transform", *International Conference on Information, Networking and Automation*, 2010, pp. V1-361 - V1-364.

[13] S. Vetova, and I. Ivanov, "Image features extraction using the dual-tree complex wavelet transform", *2nd, International Conference on Mathematical, Computational and Statistical Sciences*, 2014, pp. 277-282.

[14] W. Rasheed, G. Kang, J. Kang, J. Chun, and J. Park, "Sum of Values of Local Histograms for Image Retrieval," *Fourth International conference on Networking Computing and Advanced Information Management*, 2008, pp. 690-694.

[15] J. Wang, J. Li, and G. Wiederhold, "SIMPLIcity: Semantics-sensitive Integrated matching for Picture Libaries," *IEEE Transaction on Pattern Analysis and Machine Intelligence*, vol.23, no.9, 2001, pp. 947-963.

[16] J. Li, and J. Wang, "Autimatic Linquistic indexing of pictures by a statistical modeling approach," *IEEE Transactions on Pattern Analysis and Machine Intelligence*, vol. 25, no. 9, 2003, pp. 1075-1088.

[17] W. Rasheed, Y. An, S. Pan, I. Jeong, J. Park, J. Kang, "Image Retrieval using Maximum Frequency of Local Histogram based Color Correlogram," *International Conference Multimedia and Ubiquitous Engineering*, 2008, pp. 62-66.

[18] A. Daptardar,and J. Storer, "VQ based Image Retrieval using Color and Position Features," *Data Compression Conference*, 2008, pp. 432-441.

[19] M. Alsmadi, "An efficient similarity measure for content based image retrieval using memetic algorithm," *Egyptian Journal of Basic and Applied Sciences*, vol. 4, issue 2, 2017, pp. 112-122.

[20] I. Sumana, M. Islam, D. Zhang, and G. Lu, "Content Based Image Retrieval Using Curvelet Transform," *IEEE 10th Workshop on Multimedia Signal Processing*, 2008, pp. 11-16.

[21] B. Bama, and S. Raju, "Fourier Based Rotation Invariant Texture Features for Content Based Image Retrieval," *National Conference on Communications (NCC)*, 2010.

[22] S. Chatzichristofis, Ch. Iakovidou, Y. Boutalis, and E. Angelopoulou, "Mean Normalized Retrieval Order (MNRO). A New Content-Based Image Retrieval Performance Measure," *International Journal "Multimedia Tools and Applications*, vol. 70, issue 3, 2014, pp. 1767-1798.

[23] H. Bhuravarjula, V. Kumar, "A Novel Content Based Image Retrieval using Variance Color Moment", *International Journal of Computer and Electronics Research*, vol. 1, issue 3, 2012, pp. 93-99.

[24] S. Vetova, I. Ivanov, "Content-Based Image Retrieval Using The Dual-Tree Complex Wavelet Transform," *in Proceedings of the 2014 International Conference on Mathematics and Computers in Sciences and Industry (MCSI 2014)*, Varna, Bulgaria, September, 2014, pp. 165-170, DOI 10.1109/MCSI.2014.51.